PHYSICAL REVIEW B **83**, 220502(R) (2011)

# Nanoscale chemical phase separation in $FeTe_{0.55}Se_{0.45}$ as seen via scanning tunneling spectroscopy

Xiaobo He,[1] Guorong Li,[1] Jiandi Zhang,[1] A. B. Karki,[1] Rongying Jin,[1] B. C. Sales,[2] A. S. Sefat,[2] M. A. McGuire,[2] D. Mandrus,[3] and E. W. Plummer[1]

[1]*Department of Physics and Astronomy, Louisiana State University, Baton Rouge, Louisiana 70803, USA*

[2]*Materials Science and Technology Division, Oak Ridge National Laboratory, Oak Ridge, Tennessee 37831, USA*

[3]*Department of Materials Science, University of Tennessee, Knoxville, Tennessee 37996, USA*

(Received 7 April 2011; revised manuscript received 17 May 2011; published 6 June 2011)

Atomically resolved structural and electronic properties of $FeTe_{1-x}Se_x$ ($x = 0$ and 0.45) have been studied with scanning tunneling microscopy/spectroscopy (STM/STS). In contrast to the extreme flatness of the Te-terminated FeTe surface, nanoscale chemical phase separation between Te and Se atoms is unambiguously revealed on the surface of $FeTe_{0.55}Se_{0.45}$. A statistical counting of the two kinds of atoms has the same ratio as that in the bulk. Remarkably, there is no electronic phase separation seen in the tunneling spectroscopy. This indicates that the optimally doped superconductor is chemically inhomogeneous but electronically homogeneous, in contrast to many correlated electron materials.

DOI: 10.1103/PhysRevB.83.220502 PACS number(s): 74.70.Xa, 73.20.−r, 68.35.B−, 68.37.Ef

The discovery of superconductivity in layered iron-based materials, with transition temperatures as high as 55 K, has trigged enormous excitement and activity over the past two years.[1,2] So far, six different families of Fe-based superconductors have been discovered, all sharing a common layered structure based on square planar sheets of Fe in a tetrahedral environment with pnictogen or chalcogen anions.[3,4] Although there are some similarities to cuprates—layered structure and proximity to magnetism—Fe-based superconductors are chemically much more flexible, where superconductivity can be induced by either external pressure, isovalent substitution (chalcogen), or partial replacement for Fe by other transition metals. Thus these materials offer a new platform to explore collective behavior in complex transition metal compounds, including the pairing mechanism for superconductivity, the relevance of electron correlations[5,6] to the functionality, and the possible relationship between quantum critical behavior and superconductivity.[7]

Among all known Fe-based superconductors, the Fe chalcogenide $FeTe_{1-x}Se_x$ is structurally and chemically the simplest.[8] As shown in Fig. 1(a), the material is composed of Fe-chalcogenide slabs stacked together without any spacing layer. $Fe_{1+y}Te$ is an antiferromagnetic metal with a monoclinic structure below 65 K,[9] while $FeSe_{1-\delta}$ is a superconductor with an orthorhombic structure in the ground state.[8] What makes $FeTe_{1-x}Se_x$ particularly interesting and unique is that superconductivity results from isovalent doping of Se for Te which persists over a wide doping range ($x$).[10,11] Optimal superconducting transition occurs close to a 50% mixture of Se and Te, while other compounds require only a small amount of doping for reaching the highest $T_c$.[12] In many ways, the isovalent substitution can be viewed as a chemical pressure.

In many families of transition-metal compounds, it is believed that the chemical substitution is completely random, which is referred to as homogeneous doping. However, the electronic structure appears inhomogeneous with doping thus generating many interesting phenomena, due to strong electron correlation in these materials.[13] At present, there is very little information about the distribution of Te and Se in $FeTe_{1-x}Se_x$. To address this issue, we have used scanning tunneling microscope/spectroscopy (STM/STS) to investigate the spatial dependence of the structural and electronic properties for $FeTe_{1-x}Se_x$ with $x = 0$ and 0.45. For $x = 0.45$, Te and Se atoms can unambiguously be distinguished. Statistical analysis allows us to identify the two sites and to conclude that the distribution is not random. Interestingly, the STS measurements show that the local electronic density of states is the same everywhere in the normal state on the ordered surface (away from defects). After presenting the data we will present a model for the origin of this behavior and discuss the relationship between the size of the phase separation and the coherence length in the superconducting phase.

Single-crystal samples of $FeTe_{1-x}Se_x$ were grown by the self-flux method as described previously.[14] The sample compositions were determined using energy-dispersive x-ray spectroscopy. The measured superconducting transition temperature in the optimally doped compound $FeTe_{0.55}Se_{0.45}$ is 14 K with a specific heat jump,[15] indicating bulk superconductivity. The samples were cooled to 80 K with liquid nitrogen in a homemade low-temperature STM and then cleaved *in situ* to acquire a fresh *ab*-plane surface. Figure 1(b) shows the cleaved FeTe surface with large atomically flat terraces terminated by a step of either single- or multiple-layer step height of bulk lattice constant $c = 6.3$ Å. This assures that the crystals cleave between Fe-chalcogenide layers so that the surface is a Te layer for FeTe or a mixed Te/Se layer for a doped compound. The surface crystallographic properties are measured using low-energy electron diffraction (LEED), which reveals a highly ordered surface, the same symmetry as the bulk, and 0.07 Å compression of the Te-Fe-Te surface trilayer. The vacuum during cleavage and the STM/STS experiment was better than $5 \times 10^{-11}$ Torr. All data presented in this Rapid Communicatioin were obtained at 80 K. The STM tip was tungsten wire and checked on clean single-crystal gold *in situ* before acquiring STM/STS data on Fe chalcogenides. The tunneling conductance spectra $dI/dV$ was obtained with a lock-in amplifier. The $d^2I/dV^2$ was acquired by numerical differentiation of the measured $dI/dV$ characteristics.

 

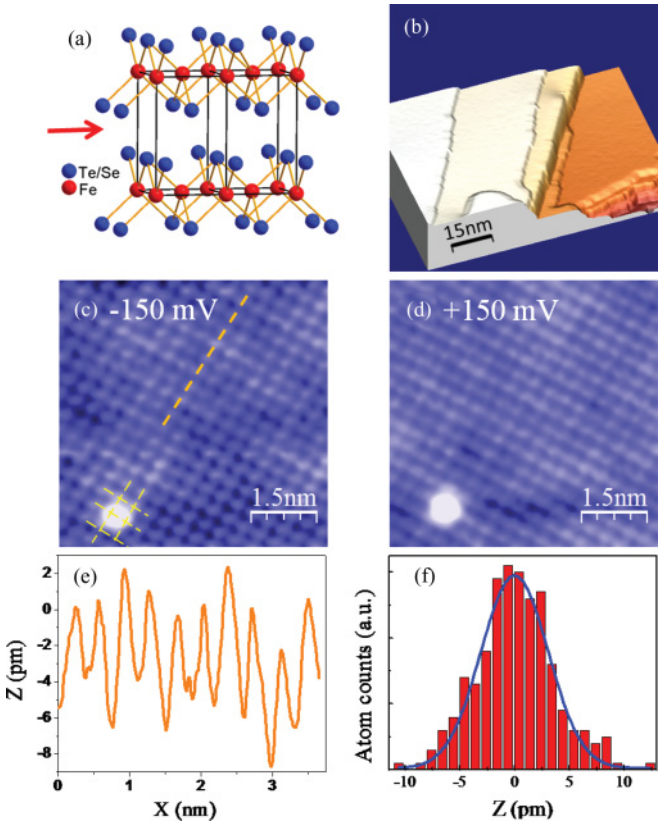


FIG. 1. (Color online) (a) Bulk crystal structure of $FeTe_{1-x}Se_x$ and the cleavage position marked by arrow. (b) 3D view of a constant-current STM topographic image of the cleaved FeTe surface showing large atomically flat terraces and steps by using a sample bias $V$ = 800 mV and tunneling current $I$ = 200 pA. Zoom-in (c) filled-state and (d) empty-state STM topographic images on the same location of cleaved FeTe surface (59 Å × 59 Å) with the tunneling current $I$ = 500 pA. (e) Line profile for the dashed line and (f) histogram of imaged atom heights in (c). The solid curve is the fitting result to a Gaussian distribution.

Figures 1(c) and 1(d) show the atomically resolved STM images with opposite-polarity bias on the same location of a cleaved FeTe surface. They are similar to previous STM studies of Fe chalcogenides,[16–18] where no reconstruction is observed. The lattice constant estimated from Fourier transform of the image is ∼3.8 Å, in good agreement with that obtained from the bulk.[14] The protrusions observed in the STM images correspond to the apical chalcogen atoms (Te) above the Fe plane in the tetrahedral building blocks. There are almost no vacancies observed on the surface. We note a few "big bright spots" that are randomly distributed on the surface. These have been assumed to be excess Fe atoms.[16,17] They are located at the bridge site of the surface lattice, which is consistent with the results of x-ray diffraction refinement[14] and density functional investigation.[19]

A conspicuous feature of the cleaved FeTe surface is its extreme flatness. Figure 1(e) presents the line profile marked in Fig. 1(c), which allows us to estimate that the surface corrugation is less than 8 pm. Different-bias STM images show similar small corrugation, although with smaller atom density (larger lattice constant), the surface corrugation of FeTe is

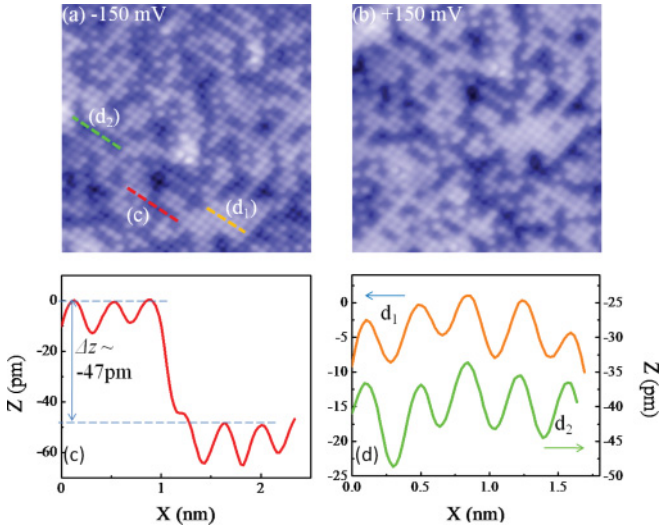


FIG. 2. (Color online) (a), (b) Constant-current STM topographic images (111 Å × 111 Å) of $FeTe_{0.55}Se_{0.45}$ surface with different bias voltages but identical tunneling current $I$ of 1.3 nA. (c) Line profile across different patches of atoms and (d) line profiles on both "bright" and "dark" atom patches marked in panel (a).

4–5 times smaller than a noble-metal surface like Cu(100),[20] indicating the itinerant characteristic of the electrons on the surface. We have carried out the statistical analysis in order to more quantitatively characterize the surface corrugation.[21] By using the mean vertical position of imaged Te atoms as a reference, a histogram of atom height ($z$) extracted from Fig. 1(c) is presented in Fig. 1(f). The appearance of a single peak in the histogram confirms a single kind of atom (Te) on the ordered FeTe surface.

We now turn to the optimally doped $FeTe_{0.55}Se_{0.45}$. The STM images with different bias voltages are shown in Figs. 2(a) and 2(b). Similar to FeTe, there are few vacancies on the surface, indicating the high crystal quality. However it is clear that there are two types of atoms, "bright" and "dark," forming irregular small patches or domains. As displayed in Fig. 2(c), there is a considerable height difference of ∼47 pm between these two kinds of patches. On the other hand, the atomic corrugation within a single patch of either bright or dark atoms [see the line profiles in Fig. 2(d)] is comparable to that of the FeTe surface. Since the adjacent atom layers (i.e., between Fe and Te/Se) are 1.48–1.72 Å apart in $FeTe_{0.55}Se_{0.45}$,[14,22,23] these dark patches of atoms should not be beneath the Fe atoms but should be within the same Te/Se layer. Note that similar images were obtained in previous STM studies on doped compounds.[17,18] Both filled-state or empty-state images show very similar contrast of the two groups of atoms. This indicates that the height difference in the STM images of $FeTe_{0.55}Se_{0.45}$ mainly comes from chemical (or crystallographic) contribution rather than an electronic effect.

To gain more insight into the nature of these two types of imaged domains, we extract the relative height of every atom in STM topographic images of cleaved $FeTe_{0.55}Se_{0.45}$. The histograms are shown in Fig. 3. Similar to the analysis of the FeTe surface, we use the mean position of bright atoms as a reference. There exists a double-peak distribution associated with the distinct two types of surface atoms, in contrast to

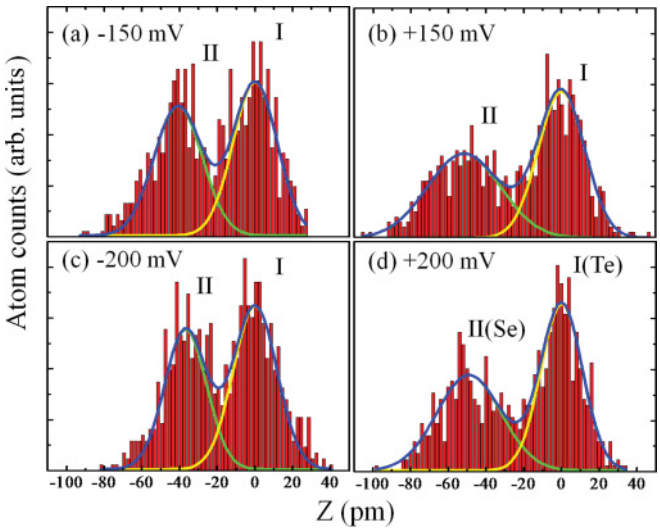


FIG. 3. (Color online) (a)–(d) Histograms of atom heights corresponding to the bias-dependent STM topographic images. The solid curves are the results by fitting to two Gaussian distributions. In each panel, the yellow (I) (light gray) and green (II) (dark gray) peaks correspond to "bright" and "dark" atoms in the image, respectively, and the blue (darkest gray) curve is the envelope sum of two peaks.

the single-peak appearance in the histogram for the FeTe surface [see Fig. 1(f)]. The solid curves in Fig. 3 are the fittings using Gaussian distributions. As listed in Table I for the fitting results, the area ratio of higher to lower peak, i.e., the ratio of bright to dark atoms, is (53.8%:46.2%). This is very close to the ratio of Te to Se in the bulk (55%:45%). We thus identify the bright atoms as Te and the dark ones as Se. As shown in Fig. 3 and Table I, the apparent height difference between Te and Se atoms in the same layer is 44.7 ± 12.1 pm in the STM images, which is larger than the results from extended x-ray absorption fine structure spectroscopy[22] and x-ray/neutron diffraction.[23,24] The larger value obtained from the STM measurements could be simply the consequence of the details of the tunneling experiment or due to the surface relaxation.

Our high-resolution STM images clearly reveal a nanophase separation between Te and Se atoms in $FeTe_{0.55}Se_{0.45}$, in sharp contrast with normally expected picture for a random alloy. To test this we counted the number of Te nearest neighbors (NN) for every Se atom in many of our STM images. We found that the NN count gives a value of ∼1.7, in contrast with the value of 2.2 expected for this concentration of a completely random alloyed $FeTe_{0.55}Se_{0.45}$. Both Te and Se atoms prefer to form small patches rather than distribute randomly. With the NN count value (∼1.7), the estimated average patch size is consistent with the experimental observation of ∼1 $nm^2$ which contains 9–10 atoms on the surface.

TABLE I. The two-Gaussian-peak fitting results of the histograms in Figs. 3(a)–3(d), including the height difference ($\Delta z$), percentage of normalized area of each peak, and their average values

| Fig. | Bias (mV) | $\Delta z$ (pm) | Peak I (%) | Peak II (%) |
|---|---|---|---|---|
| 3(a) | −150 | −40.9 | 54.6 | 45.4 |
| 3(b) | +150 | −51.8 | 53.2 | 46.8 |
| 3(c) | −200 | −36.9 | 54.4 | 45.6 |
| 3(d) | +200 | −49.1 | 52.8 | 47.2 |
| Ave. | | −44.7±12.0 | 53.8±1.5 | 46.2±1.5 |

This configuration would lead to a local inhomogeneity in chemical pressure, which could drive a local structural change. In the ground state, the structure of FeTe is monoclinic while the structure of FeSe is orthorhombic. The central question is, do the electronic properties including superconductivity respond to the local chemical (crystallographic) inhomogeneity? To gain insight into this critical issue, we have measured the $dI/dV$ spectra on individual Te and Se atoms, as well as the average $dI/dV$ spectra on their associated patches. The results are shown in Fig. 4 for both $FeTe_{0.55}Se_{0.45}$ and FeTe surfaces. Note that in the energy window of ±100 mV around the Fermi surface [Figs. 4(a) and 4(b)], all the individual $dI/dV$ taken on Te and Se sites on the $FeTe_{0.55}Se_{0.45}$ surface are indistinguishable. To further confirm this, we have taken many more spectra at the surface on the same STM image [Fig. 4(a)] and averaged all the spectra taken from Te (Se) atoms or patches, respectively. The two averaged $dI/dV$ spectra, one from Te and other from Se, are identical, as shown in Fig. 4(c), independent of the local chemical environment. The earlier report of spatial variations in the $dI/dV$ spectra at high energy[17] is likely due to the excess Fe. For comparison, the tunneling spectra of the FeTe surface is also presented. The pronounced feature in the $dI/dV$ of FeTe is the enhanced local density of states (LDOS) around 20 mV as compared with $FeTe_{0.55}Se_{0.45}$.

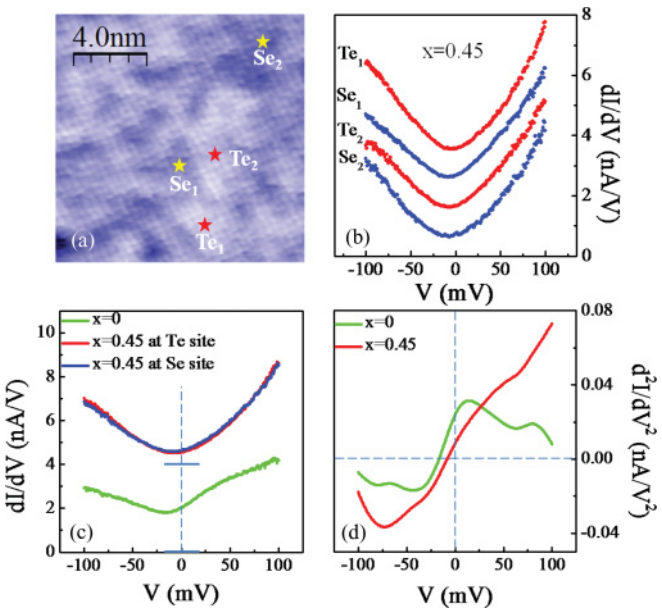


FIG. 4. (Color online) (a) A 128 Å × 128 Å constant-current STM topographic image on the $FeTe_{0.55}Se_{0.45}$ surface. $I = 1.5$ nA, $V = -100$ mV. (b) Tunneling spectra taken at several Te and Se sites indicated in (a). Curves are vertically shifted for clarity. (c) Averaged $dI/dV$ spectra at Te and Se sites on $FeTe_{0.55}Se_{0.45}$ surface in (a) and on FeTe surface. The spectra are also shifted for clarity, with the zero value of $dI/dV$ marked by solid lines. (d) The corresponding $d^2I/dV^2$ curves acquired by numerical differentiation of the measured $dI/dV$ spectra in (c). All the data were taken at 80 K.

The difference in the electronic properties between them is best displayed in Fig. 4(d) where the $d^2I/dV^2$ spectra are presented. The most obvious differences are the position at the zero bias ($V = 0$) and the peak around 20 mV in the parent compound.

The data presented here reveal a surprising feature: inhomogeneous chemical distribution gives rise to homogeneous electronic behavior. What has been expected for many doped correlated electron materials is just the opposite: chemical homogeneity but electronic and magnetic phase separation.[13] Electronic homogeneity and very small corrugation in the STM topograph coupled with the nearly homogeneous superconducting gap[17,18] indicate that this compound is closer to an itinerant metal than to a highly correlated material. Superconductivity in this compound with nanoscale chemical phase separation must be a consequence of the fact that the sizes of chemical patches are smaller than the superconducting coherence length resulting in a homogenous superconducting gap.

What may have occurred for $x \sim 0.5$ is that Te and Se nanoscale phases compensate each other in the trilayered structure [see Fig. 1(a)]. That is, everywhere that we see a Te patch on the surface, there could be a Se patch underneath the Fe in the third layer. Thus, the Se/Te concentration in the triplet layer system is nearly homogeneous. If this is the case, the follow-up question is, what is the chemical and electronic behavior in doped $FeTe_{1-x}Se_x$ when $x$ is away from ~50%? For example, electrical resistivity shows both weakly localized electronic behavior and filamentary superconductivity for $0.1 < x < 0.3$.[11] Is this caused by large-scale chemical inhomogeneity which leads to electronic inhomogeneity or by random chemical distribution generating strong scattering which leads to weak localization? This can only be answered by further STM/STS investigation.

In summary, scanning tunneling microscopy and spectroscopy have been performed with Fe chalcogenides FeTe and $FeTe_{0.55}Se_{0.45}$. In both cases, the cleaved surfaces are chalcogen terminations without reconstruction. A very small corrugation is measured for the cleaved FeTe surface. Mixed Te and Se atoms in $FeTe_{0.55}Se_{0.45}$ can be identified in STM topography by statistical analysis, consistent with that found in bulk. Furthermore, direct evidence of local chemical inhomogeneity in the Fe-Te/Se layer of $FeTe_{0.55}Se_{0.45}$ is found with significant height difference between Te and Se atoms, leading to larger surface corrugation. In contrast to the nanoscale chemical phase separation, the local electronic properties revealed by tunneling spectroscopy show no sign of inhomogeneity.

The authors are grateful to Y. Li and J. Teng for the initial technical assistance. The work at LSU was supported by NSF DMR-1002622. X.H. received the support from DOE DE-SC0002136. The work at ORNL was sponsored by the Materials Sciences and Engineering Division (A.S.S., M.A.M., and B.C.S.), US Department of Energy, under Contract No. DE-AC05-000R22725 with UT-Battle, LLC.

[1] Y. Kamihara, T. Watanabe, M. Hirano, and H. Hosono, J. Am. Chem. Soc. **130**, 3296 (2008).
[2] D. C. Johnston, Adv. Phys. **59**, 803 (2010).
[3] S. J. Paglione and R. L. Greene, Nature Phys. **6**, 645 (2010).
[4] J. Guo, S. Jin, G. Wang, S. Wang, K. Zhu, T. Zhou, M. He, and X. Chen, Phys. Rev. B **82**, 180520(R) (2010).
[5] M. M. Qazilbash, J. J. Hamlin, R. E. Baumbach, L. Zhang, D. J. Singh, M. B. Maple, and D. N. Basov, Nature Phys. **5**, 647 (2009).
[6] A. Tamai, A. Y. Ganin, E. Rozbicki, J. Bacsa, W. Meevasana, P. D. C. King, M. Caffio, R. Schaub, S. Margadonna, K. Prassides, M. J. Rosseinsky, and F. Baumberger, Phys. Rev. Lett. **104**, 097002 (2010).
[7] J. Dai, Q. Si, J. Zhu, and E. Abrahams, Proc. Natl. Acad. Sci. USA **106**, 4118 (2009).
[8] F. C. Hsu, J. Luo, K. Yeh, T. Chen, T. Huang, P. M. Wu, Y. Lee, Y. Huang, Y. Chu, D. Yan, and M. Wu, Proc. Natl. Acad. Sci. USA **105**, 14262 (2008).
[9] W. Bao, Y. Qiu, Q. Huang, M. A. Green, P. Zajdel, M. R. Fitzsimmons, M. Zhernenkov, S. Chang, M. Fang, B. Qian, E. K. Vehstedt, J. Yang, H. M. Pham, L. Spinu, and Z. Q. Mao, Phys. Rev. Lett. **102**, 247001 (2009).
[10] A. V. Balatsky and D. Parker, Physics **2**, 59 (2009).
[11] T. J. Liu, J. Hu, B. Qian, D. Fobes, Z. Q. Mao, W. Bao, M. Reehuis, S. A. J. Kimber, K. Prokes, S. Matas, D. N. Argyriou, A. Hiess, A. Rotaru, H. Pham, L. Spinu, Y. Qiu, V. Thampy, A. T. Savici, J. A. Rodriguez, and C. Broholm, Nature Mater. **9**, 718 (2010).
[12] N. Ni, M. E. Tillman, J.-Q. Yan, A. Kracher, S. T. Hannahs, S. L. Bud'ko, and P. C. Canfield, Phys. Rev. B **78**, 214515 (2008).
[13] E. Dagotto, Science **309**, 257 (2005).
[14] B. C. Sales, A. S. Sefat, M. A. McGuire, R. Y. Jin, D. Mandrus, and Y. Mozharivskyj, Phys. Rev. B **79**, 094521 (2009).
[15] H. A. Mook, M. D. Lumsden, A. D. Christianson, S. E. Nagler, B. C. Sales, R. Jin, M. A. McGuire, A. S. Sefat, D. Mandrus, T. Egami, and C. dela Cruz, Phys. Rev. Lett. **104**, 187002 (2010).
[16] F. Massee, S. de Jong, Y. Huang, J. Kaas, E. van Heumen, J. B. Goedkoop, and M. S. Golden, Phys. Rev. B **80**, 140507(R) (2009).
[17] T. Kato, Y. Mizuguchi, H. Nakamura, T. Machida, H. Sakata, and Y. Takano, Phys. Rev. B **80**, 180507(R) (2009).
[18] T. Hanaguri, S. Niitaka, K. Kuroki, and H. Takagi, Science **328**, 474 (2010).
[19] L. Zhang, D. J. Singh, and M. H. Du, Phys. Rev. B **79**, 012506 (2009).
[20] Z. Q. Zou, Z. C. Dong, A. S. Trifonov, and H. Nejo, J. Vac. Sci. Technol. B **20**, 1567 (2002).
[21] I. Horcas, R. Fernandez, J. M. Gomez-Rodriguez, J. Colchero, J. Gomez-Herrero, and A. M. Baro, Rev. Sci. Instrum. **78**, 013705 (2007).
[22] B. Joseph, A. Iadecola, A. Puri, L. Simonelli, Y. Mizuguchi, Y. Takano, and N. L. Saini, Phys. Rev. B **82**, 020502(R) (2010).
[23] M. Tegel, C. Lohnert, and D. Johrendt, Solid State Commun. **150**, 383 (2010).
[24] D. Louca, K. Horigane, A. Llobet, R. Arita, S. Ji, N. Katayama, S. Konbu, K. Nakamura, T.-Y. Koo, P. Tong, and K. Yamada, Phys. Rev. B **81**, 134524 (2010).